

Gamma rays and neutrinos from a cosmic ray source in the Galactic Center region

A. D. Supanitsky

*Instituto de Astronomía y Física del Espacio (IAFE), CONICET-UBA,
CC 67, Suc. 28, C1428ZAA Buenos Aires, Argentina.**

(Dated: August 1, 2018)

The center of the our Galaxy is a region where very energetic phenomena take place. In particular powerful cosmic ray sources can be located in that region. The cosmic rays accelerated in these sources may interact with ambient protons and/or low energy photons producing gamma rays and neutrinos. The observation of these two types of secondary particles can be very useful for the identification of the cosmic ray sources and for the understanding of the physical processes occurring during acceleration.

Motivated by the excess in the neutrino spectrum recently reported by the IceCube Collaboration, we study in detail the shape of the gamma ray and neutrino spectra originated from the interaction of cosmic ray protons with ambient protons for sources located in the Galactic Center region. We consider different models for proton acceleration and study the impact on the gamma ray and neutrino spectra. We also discuss the possibility to constrain and even identify a particular neutrino source by using the information given by the gamma ray spectrum taking advantage of the modification of the spectral shape, caused by the interaction of the gamma rays with the photons of the radiation field present in the interstellar medium, which strongly depends on the source distance.

I. INTRODUCTION

Gamma rays and neutrinos can be generated in cosmic ray sources due to the interaction of the cosmic rays with ambient photons and/or protons. Powerful cosmic ray accelerators can be located in the Galactic Center region; therefore, the observation of gamma rays and neutrinos coming from the Galactic Center is of great importance for the identification and understanding of the Galactic cosmic ray sources. It is worth noting that, in contrast with charged cosmic rays, these two types of secondary particles are not deviated by the magnetic fields present in the interstellar medium and then they point back to its source.

The IceCube Collaboration has recently reported the observation of 28 neutrino events in the energy range from 30 TeV to 1.2 PeV [1, 2], while only $10.6^{+4.6}_{-3.9}$ events were expected considering a conventional atmospheric neutrino background. This corresponds to a $\sim 4.3 \sigma$ excess. Despite the large angular uncertainty of these events ($\sim 10^\circ$), we can observe that 5 of the 28 events come from the Galactic Center region. However, there is a degeneracy about the origin of these neutrinos because they can also originate outside our Galaxy. It has been pointed out that the gamma ray flux associated with the neutrino flux can be useful to constrain or even identify the candidate neutrino sources [3–6]. In particular, in Refs. [7, 8] it is found that the gamma ray data taken by Fermi LAT at lower energies are consistent with a Galactic origin of these five events. However, the upper limits on the diffuse gamma ray flux obtained by different experiments at higher energies disfavor this hypothesis [6].

On the other hand, the region in the cosmic ray energy spectrum where the transition from the Galactic to extragalactic cosmic rays takes place is still unknown (see Ref. [9] for a review). Two possible regions for this transition are the second knee, a steepening of the spectrum which is given at an energy of ~ 0.5 EeV, and the ankle, a hardening of the spectrum placed at an energy of ~ 3 EeV. In Ref. [4] it has been pointed out that the identification of Galactic neutrino sources and the observation of their spectra can contribute to finding the region where the transition from Galactic to extragalactic cosmic rays takes place. This is due to the fact that the end of the neutrino energy spectrum is correlated with the maximum energy at which the cosmic rays are accelerated in the source. Following Ref. [4], the observation of the end of the neutrino spectrum, of a given Galactic source, at $E_\nu^{max} \cong 1$ PeV favors the scenario in which the transition takes place in the second knee region, whereas the observation of $E_\nu^{max} \cong 8 - 10$ PeV favors the scenario in which the transition is given at the ankle region.

The most probable mechanism for the production of gamma rays and neutrinos in Galactic cosmic ray sources is the interaction of cosmic rays with ambient protons [3]. In this work we study in detail the shape of the gamma ray and neutrino spectra that originate from the proton-proton interaction in Galactic cosmic ray sources placed in the Galactic Center region, which is motivated by the recent IceCube results. We consider different shapes of the proton spectrum based on acceleration models. We also consider the values for the maximum energy of protons corresponding to the Galactic to extragalactic transition in the second knee region and in the ankle region. The propagation of the gamma rays and neutrinos from the Galactic Center to the Solar System is included in these calculations. While neutrinos suffer flavor oscillation during propagation, gamma rays can interact with the photons of the Galactic interstellar radiation field

* supanitsky@iafe.uba.ar

(ISRF) and the cosmic microwave background (CMB) which is the most important one [10]. In particular, we find that the ratio between the neutrino and gamma ray spectra depends on the cosmic ray proton spectrum, which can be used to study the conditions under which the cosmic ray protons are accelerated in the source. Finally, we study the possibility to discriminate between the Galactic and extragalactic origins of a neutrino spectrum observed in the direction of the Galactic Center by observing the associated gamma ray flux, which in principle will be possible with the planned high energy gamma ray observatories.

II. GAMMA RAYS AND NEUTRINOS INJECTED BY A COSMIC RAY SOURCE

Gamma rays and neutrinos can be produced as a result of the interaction of the cosmic rays with ambient protons present in the sources. Gamma rays are mainly produced by the decay of neutral pions; η mesons also contribute to the gamma ray flux. The generation of neutrinos is dominated by the decay of charged pions. Positive (negative) charged pions mainly decay into an antimuon and a muon (antimuon) neutrino,

$$\begin{aligned}\pi^+ &\rightarrow \mu^+ + \nu_\mu, \\ \pi^- &\rightarrow \mu^- + \bar{\nu}_\mu.\end{aligned}$$

The subsequent decay of the muons and antimuons produces more neutrinos,

$$\begin{aligned}\mu^+ &\rightarrow e^+ + \nu_e + \bar{\nu}_\mu, \\ \mu^- &\rightarrow e^- + \bar{\nu}_e + \nu_\mu.\end{aligned}$$

It is believed that the Galactic cosmic rays are accelerated principally at supernova remnants (see e. g. Ref. [11]) by means of the first order Fermi mechanism. Also, the experimental evidence indicates that the injected composition of the Galactic sources is dominated by protons [12]. The spectrum of protons that escape from the acceleration region accelerated via the first order Fermi mechanism, without taking account of energy losses, can be written as

$$\begin{aligned}\Phi_p(E_p) &= A E_p^{-\gamma} \left(1 + \left(\frac{E_p}{E_{max}} \right)^{2\delta} \right) \\ &\times \exp \left(-\frac{\gamma-1}{2\delta} \left(\frac{E_p}{E_{max}} \right)^{2\delta} \right),\end{aligned}\quad (1)$$

where A is a normalization constant, γ is the spectral index, E_{max} refers to the maximum energy which indicates the end of the spectrum (note that protons can be accelerated to higher energies than E_{max}), and δ comes from the energy dependence of the diffusion coefficient in the acceleration region, $k \propto E^\delta$ (see Appendix A for details).

Cosmic rays can suffer energy losses during the acceleration process due to the presence of strong magnetic fields

and ambient low energy photons [13, 14]. The spectrum near its end can have different shapes, including pileups and sudden cutoffs, depending on the type of energy loss dominating in the acceleration region. Then, in the subsequent analyses a proton spectrum with a sudden cutoff in E_{max} is also considered,

$$\Phi_p(E_p) = A \begin{cases} E_p^{-\gamma} & E_p \leq E_{max} \\ 0 & E_p > E_{max} \end{cases}. \quad (2)$$

Figure 1 shows the proton spectra for $\gamma = 2$ and for $\delta = 1/3$ (Kolmogorov spectrum), $\delta = 1/2$ (Kraichnan spectrum), and $\delta = 1$ (completely disordered field) [14]. The spectrum corresponding to the sudden cutoff is also shown. The maximum energy considered is $E_{max} = 2 \times 10^4$ TeV, which corresponds to the transition between the Galactic and extragalactic cosmic rays in the region of the second knee. As expected, the steepening of the spectra is more pronounced for increasing values of δ .

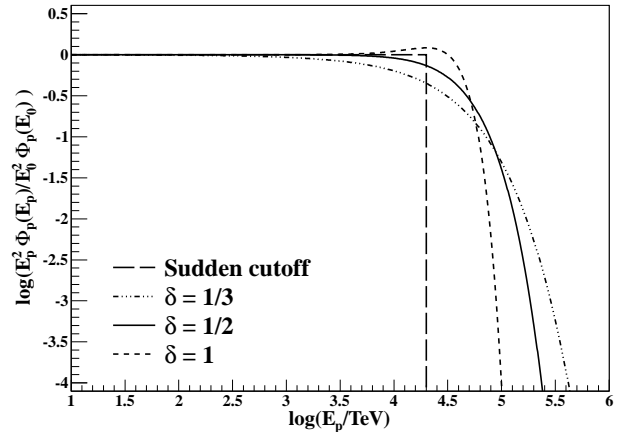


FIG. 1. Logarithm of the proton spectra multiplied by E^2 as a function of the logarithm of the proton energy. The spectral index considered is $\gamma = 2$ and the maximum energy is $E_{max} = 2 \times 10^4$ TeV. The spectra multiplied by E^2 are normalized at an energy $E_0 = 10$ TeV.

Given the proton spectrum the spectra of gamma rays and neutrinos generated by the interaction with the ambient protons are calculated following Ref. [15]. In that work the proton-proton interaction was simulated by using the hadronic interaction model Sibyll 2.1 [16]. The gamma ray spectrum is calculated from

$$\Phi_\gamma^0(E_\gamma) = C \int_{E_\gamma}^{\infty} \frac{dE_p}{E_p} \sigma_{inel}(E_p) \Phi_p(E_p) F_\gamma \left(\frac{E_\gamma}{E_p}, E_p \right), \quad (3)$$

where C is a normalization constant and σ_{inel} is the proton-proton inelastic cross section. σ_{inel} and F_γ are taken from Ref. [15]. The neutrino and antineutrino spectra are obtained in a similar way, and the corresponding functions are also taken from Ref. [15].

Figure 2 shows the gamma ray and neutrino¹ spectra at the source for $\gamma = 2$, $E_{max} = 2 \times 10^4$ TeV, and $\delta = 1/2$. Note that the results obtained in this work are in very good agreement with the ones obtained in Ref. [17]. From Fig. 2 it can be seen that the gamma

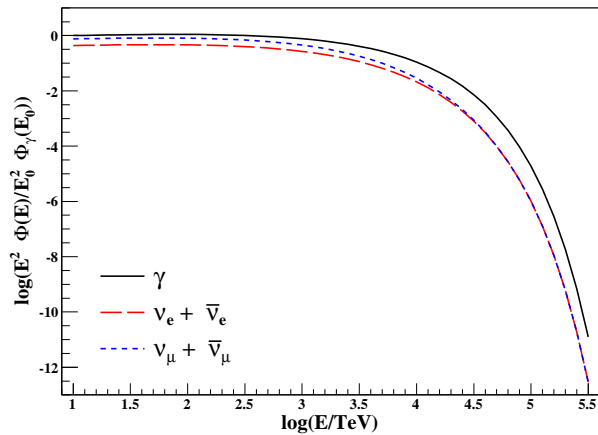


FIG. 2. Logarithm of the gamma ray and neutrino spectra multiplied by E^2 as a function of the logarithm of the energy for $\gamma = 2$, $E_{max} = 2 \times 10^4$ TeV, and $\delta = 1/2$. Also in this case $E_0 = 10$ TeV.

ray spectrum is larger than the one corresponding to the electron neutrino and muon neutrino. Also, the end of the neutrino spectra takes place at a smaller energy than the one corresponding to gamma rays.

III. GAMMA RAYS AND NEUTRINOS AT EARTH

A. Precise calculation

Gamma rays and neutrinos produced at a given source propagate through the interstellar medium to reach the Earth. The electron and muon neutrinos oscillate during propagation; therefore, the flavor ratio observed at the Earth is different from the one in the source. It is believed that the neutrino oscillations originate from the fact that the flavor states, $|\nu_\alpha\rangle$ with $\alpha = e, \mu, \tau$, are not the mass eigenstates, $|\nu_j\rangle$ with $j = 1, 2, 3$. The flavor and the mass basis are related by [18]

$$|\nu_\alpha\rangle = \sum_{j=1}^3 U_{\alpha j}^* |\nu_j\rangle, \quad (4)$$

where U is a unitary matrix which can be parametrized by the mixing angles θ_{12} , θ_{23} , and θ_{13} and a CP violating

phase δ_{CP} . The transition probability can be written as [18]

$$P_{\nu_\alpha \rightarrow \nu_\beta} = \sum_{j=1}^3 |U_{\alpha j}|^2 |U_{\beta j}|^2. \quad (5)$$

In the so-called tribimaximal mixing approximation [19] the parameters of the mixing matrix are taken as $\theta_{12} = \arcsin(1/\sqrt{3})$, $\theta_{23} = \pi/4$, $\theta_{13} = 0$, and $\delta_{CP} = 0$. By using this approximation it can be seen that a flavor ratio 1 : 2 : 0 in the source goes to 1 : 1 : 1 after propagation. In this work a more precise estimation of the mixing angles is used in which θ_{13} is different from zero [20]: $\sin^2(2\theta_{12}) = 0.857$, $\theta_{23} = \pi/4$, and $\sin^2(2\theta_{13}) = 0.096$. It is also assumed that $\delta_{CP} = 0$. By using this new estimation of the parameters the flavor ratio 1 : 2 : 0 goes to 1.05 : 0.99 : 0.95, which is very close to the tribimaximal mixing approximation. Therefore, the propagated spectra are calculated from

$$\begin{pmatrix} \Phi_{\nu_e} \\ \Phi_{\nu_\mu} \\ \Phi_{\nu_\tau} \end{pmatrix} = \mathbf{P} \begin{pmatrix} \Phi_{\nu_e}^0 \\ \Phi_{\nu_\mu}^0 \\ \Phi_{\nu_\tau}^0 \end{pmatrix} \quad (6)$$

where the elements of the \mathbf{P} matrix are given by $P_{\alpha\beta} = P_{\nu_\alpha \rightarrow \nu_\beta}$ and $\Phi_{\nu_\alpha}^0$ are the neutrino spectra at the source. Note that in this case $\Phi_{\nu_\tau}^0 = 0$.

Gamma rays interact with photons of different backgrounds when they propagate from the source to the Earth; the most important ones are the CMB and the ISRF [10]. The most important process at the energies considered is the electron-positron pair production. Figure 3 shows the mean free path of photons, λ_γ , as a function of energy for the CMB. The calculation has been done following Ref. [21]. From the figure it can be seen that for energies of order of 1 PeV $\lambda_\gamma \sim 9$ kpc, which is very close to the distance from the Solar System to the Galactic Center ($D = 8.5$ kpc). Therefore, at these energies the attenuation in the CMB becomes quite important.

The attenuation factor is given by $T(E_\gamma, D) = \exp(-\tau(E_\gamma, D))$, where D is the distance from the source to the Earth and

$$\tau(E_\gamma, D) = \int_0^D \frac{d\ell}{\lambda_\gamma(E_\gamma, \ell)}. \quad (7)$$

Thus, the gamma ray flux at the Earth is given by

$$\Phi_\gamma(E_\gamma) = \frac{T(E_\gamma, D) \Phi_\gamma^0(E_\gamma)}{4\pi D^2}. \quad (8)$$

Figure 4 shows the attenuation factor for the CMB and ISRF (taken from Ref. [10]) as a function of the energy for two different positions of the source: One is placed at the Galactic Center and the other at 4 Mpc from the Solar System in the direction of the Galactic Center. The attenuation factor for the ISRF is taken from Ref. [10]; the one corresponding to the extragalactic source is obtained by integrating $\lambda_\gamma^{-1}(E_\gamma, \ell)$ from a distance of 28.5

¹ Hereafter, neutrino spectrum will refer to the sum of the neutrino and antineutrino spectra of a given flavor.

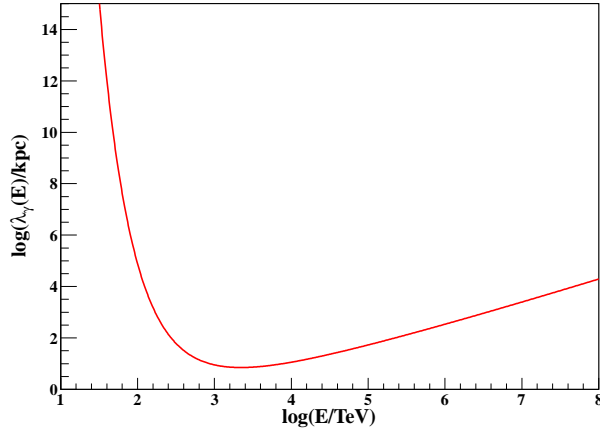


FIG. 3. Logarithm of the mean free path of gamma rays as a function of the logarithm of the primary energy for electron-positron pair production in the CMB.

kpc in the direction of the Galactic Center (see Eq. (7)). It can be seen that the attenuation caused by the interaction with the CMB photons is more important than that corresponding to the ISRF.

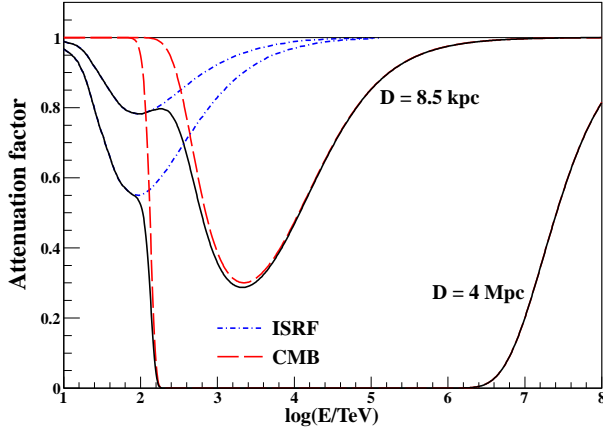


FIG. 4. Attenuation factor of gamma rays as a function of the logarithm of energy. The photon backgrounds considered are the CMB and the ISRF. One source is placed at the Galactic Center ($D = 8.5$ kpc), and the other is placed at $D = 4$ Mpc in the direction of the Galactic Center.

The top panel of Fig. 5 shows the gamma ray and neutrino spectra at the Earth for a Galactic cosmic ray source, like the one considered in Sect. II ($\gamma = 2$, $E_{max} = 2 \times 10^4$ TeV, and $\delta = 1/2$), located in the Galactic Center. In this figure the effects of the attenuation in the gamma ray spectra are evident. Also, the neutrino spectra for the different flavors become similar after propagation. The bottom panel of Fig. 5 shows the ratio $R_{\nu/\gamma}$ of the neutrino spectra to the gamma ray spectrum. It can be seen that it is not constant in a large energy range due to the attenuation suffered by the gamma rays and the different ends of the neutrino and gamma ray spectra. In particular, the first maximum of $R_{\nu/\gamma}$ corresponds to

the attenuation of the gamma rays in the ISRF, whereas the second and larger one corresponds to the attenuation in the CMB.

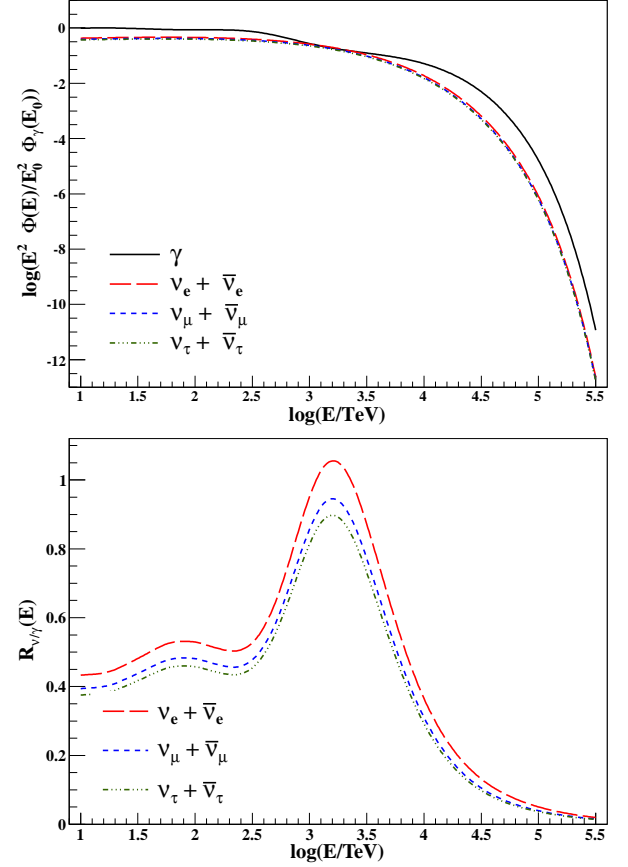


FIG. 5. Top panel: Logarithm of the gamma ray and neutrino spectra at the Earth multiplied by E^2 as a function of the logarithm of the energy for a cosmic ray source located at the Galactic Center. Bottom panel: Ratio of the neutrino spectra to the gamma ray spectrum as a function of the logarithm of the energy. The parameters used are $\gamma = 2$, $E_{max} = 2 \times 10^4$ TeV, and $\delta = 1/2$.

The shape of the end of the gamma ray and neutrino spectra depends on the shape of the proton spectrum. Figure 6 shows the gamma ray and the total neutrino spectra (summed over all flavors) at the Earth as a function of energy for the different values of δ considered and for the case in which the proton spectrum presents a sudden cutoff. The maximum energy of the proton spectrum is $E_{max} = 2 \times 10^4$ TeV. As expected, when the proton spectrum ends faster, the gamma ray and the neutrino spectra also end faster.

Figure 7 shows the ratio between the total neutrino spectrum and the gamma ray spectrum as a function of energy, corresponding to the spectra shown in Fig. 6. It can be seen that $R_{\nu/\gamma}$ presents two maxima; as mentioned above, the first one corresponds to the attenuation due to the interaction of the gamma rays with the photons of the ISRF and the second one to the CMB.

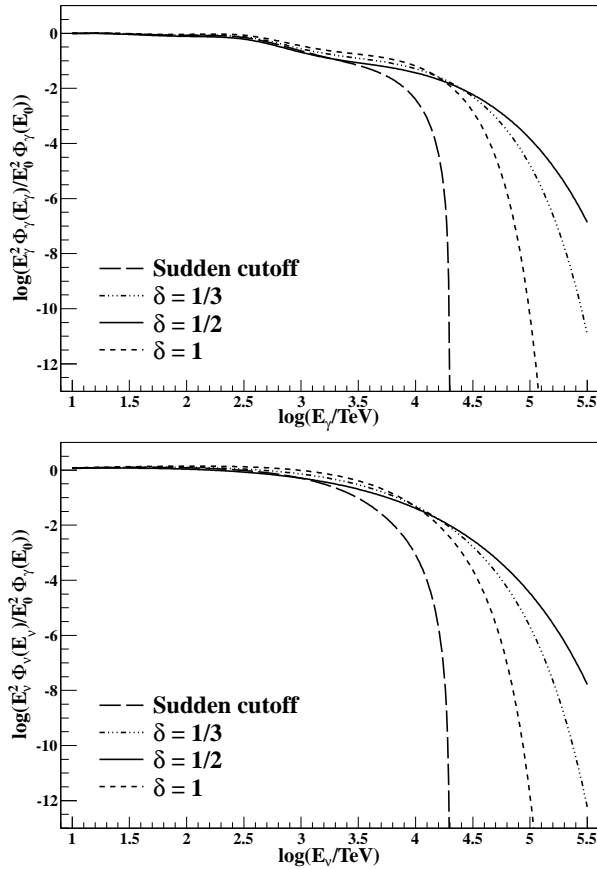


FIG. 6. Logarithm of the gamma ray (top panel) and neutrino (bottom panel) spectra at the Earth multiplied by E^2 as a function of the logarithm of the energy for a cosmic ray source located at the Galactic Center and for the different cases of the proton spectrum considered. The maximum energy of the proton spectrum is $E_{max} = 2 \times 10^4$ TeV.

Also, the shape of $R_{\nu/\gamma}$ depends on the type of proton spectrum considered, which can be useful, from the observational point of view, to study the end of the proton spectrum at the source, which is intimately related to the diffusion coefficient and the energy losses suffered by protons in the acceleration region.

The gamma ray and neutrino spectra are modified when the maximum energy of the accelerated protons increases. Figure 8 shows the ratio between the total neutrino spectrum and the gamma ray spectrum as a function of energy for the maximum energy of the proton spectrum $E_{max} = 1.2 \times 10^5$ TeV, which corresponds to the case in which the transition between the Galactic and extragalactic cosmic rays is given in the ankle region. It can be seen that in this case $R_{\nu/\gamma}$ is larger than one corresponding to the case considered above. This is due to the fact that, in this case, the region in which the attenuation on the CMB is more important ($E_\gamma \sim 10^{3.3}$ TeV), the gamma ray and neutrino spectra approximately follow the shape of the proton spectrum; i.e. the end of the spectra is given at higher energies. Also in this case,

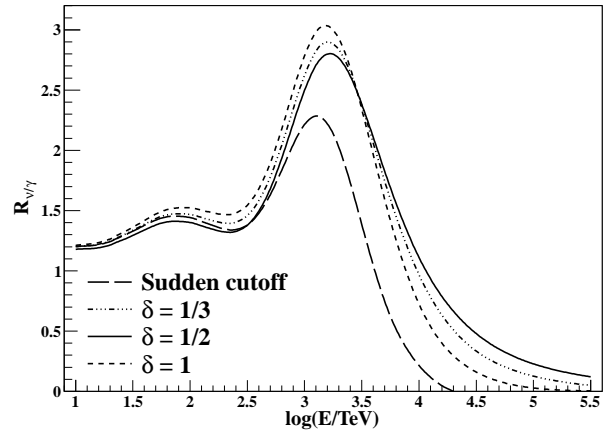


FIG. 7. Ratio between the neutrino spectrum and the gamma ray spectrum as a function of the logarithm of the energy for a cosmic ray source located in the Galactic Center region for the different cases of the proton spectrum considered. The maximum energy of the proton spectrum is $E_{max} = 2 \times 10^4$ TeV.

the ratio can be useful to study the end of the proton spectrum at the source, which is related to the physical conditions under which the protons are accelerated.

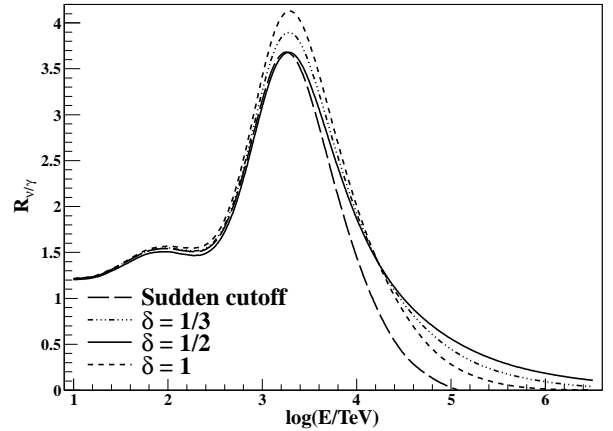


FIG. 8. Ratio between the neutrino spectrum and the gamma ray spectrum as a function of the logarithm of the energy for a cosmic ray source located in the Galactic Center region for the different cases of the proton spectrum considered. The maximum energy of the proton spectrum is $E_{max} = 1.2 \times 10^5$ TeV.

It can be seen that by increasing the spectral index γ , the steepening of the gamma ray and neutrino spectra takes place at lower energies, which makes $R_{\nu/\gamma}$ decrease.

B. Approximate calculation

It is quite common to calculate the gamma ray spectrum from the neutrino spectrum (and the other way around), making use of several approximations (see, for

instance, Ref. [6]). In this section the accuracy of this approximation is studied by means of the numerical calculations presented above. In proton-proton collisions π^0 , π^+ , and π^- are created with the same multiplicity. As a result of the decay of charged pions and the subsequent muon or antimuon decay four particles are created; three of those are neutrinos, and then $E_\nu \cong E_\pi/4$. In the case of neutral pion decay two photons are created; then $E_\gamma \cong E_\pi/2$. Therefore, $E_\nu \cong E_\gamma/2$, and the differential flux of gamma rays can be obtained from [6]

$$\begin{aligned}\Phi_\gamma(E_\gamma) &\cong \frac{1}{3} \sum_\alpha \Phi_{\nu_\alpha + \bar{\nu}_\alpha} \left(\frac{E_\gamma}{2} \right) \frac{dE_\nu}{dE_\gamma} \\ &\cong \frac{1}{6} \sum_\alpha \Phi_{\nu_\alpha + \bar{\nu}_\alpha} \left(\frac{E_\gamma}{2} \right),\end{aligned}\quad (9)$$

where $\alpha = e, \mu, \tau$. Here the effects of the propagation of gamma rays in the interstellar medium are not taken into account in order to better compare the spectral shape of the numerical calculation and the approximation.

Figure 9 shows the gamma ray spectrum as a function of the energy calculated as in Sec. III A (solid line) and from the neutrino spectra, also calculated as in Sec. III A, by using Eq. (9) (dashed line) for $\gamma = 2$, $E_{max} = 2 \times 10^4$ TeV, and $\delta = 1/2$. The approximation underestimates the gamma ray spectrum at lower energies and overestimates the spectrum at higher energies. Note that the larger differences between the approximated calculation and the numerical one are given at high energies, in the region at the end of the spectrum. In particular, the approximated spectrum is less steep in that energy region, which makes the difference between the approximated spectrum and the numerical one to increase with energy.

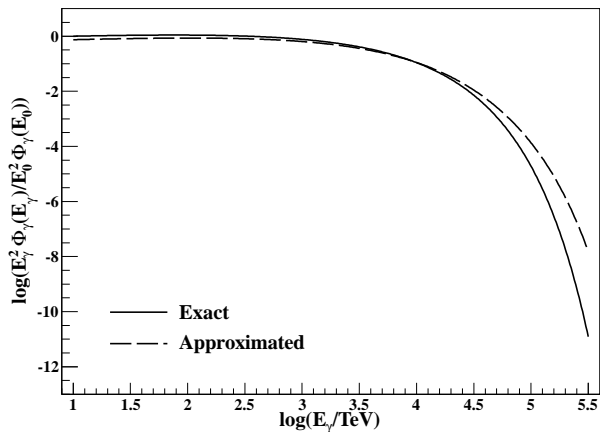


FIG. 9. Logarithm of the gamma ray spectra multiplied by E^2 as a function of the logarithm of the energy for $\gamma = 2$, $E_{max} = 2 \times 10^4$ TeV, and $\delta = 1/2$. The solid line corresponds to the numerical calculation and the dashed line to the approximation based on Eq. (9).

In order to quantify these differences let us introduce

the following parameter,

$$\varepsilon(\Phi_\gamma)(E) = 1 - \frac{\Phi_\gamma^{app}(E)}{\Phi_\gamma(E)}, \quad (10)$$

where $\Phi_\gamma^{app}(E)$ is the approximated spectrum and $\Phi_\gamma(E)$ is the one obtained numerically. Figure 10 shows the relative error $\varepsilon(\Phi_\gamma)$ as a function of energy for the four cases of the proton spectrum considered with $\gamma = 2$ and $E_{max} = 2 \times 10^4$ TeV. At lower energies the differences between the approximated spectra and the numerical one are smaller than $\sim 26\%$. The larger differences take place in the region at the end of the gamma ray spectra because, as mentioned above, the approximated spectra is less steep than the numerical one. Note that in all cases considered, the behavior of the relative error is qualitatively similar; in the region corresponding to the end of the spectra, the absolute value of the relative error increases with energy, reaching values of the order of 100% very fast. Note also that the approximation underestimates the spectrum at lower energies and overestimates it in the region corresponding to the end of the spectrum, i.e. $\varepsilon(\Phi_\gamma)$ changes its sign at a given energy depending on the proton spectrum considered.

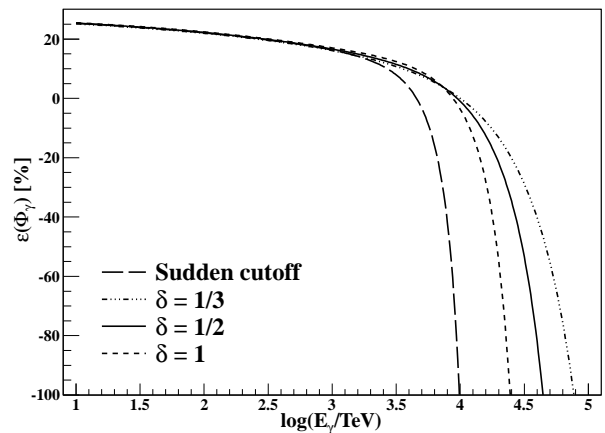


FIG. 10. Relative error of the approximated spectra as a function of the logarithm of the energy for $\gamma = 2$ and $E_{max} = 2 \times 10^4$ TeV.

IV. GALACTIC VERSUS EXTRAGALACTIC ORIGIN OF THE OBSERVED NEUTRINO SPECTRUM

It is not possible to elucidate the origin of neutrinos coming from the Galactic Center region with just the observation of their energy spectrum and arrival direction distribution. There is a degeneracy; these neutrinos can originate in other regions of the Galaxy or even outside the Galaxy. This degeneracy can be broken by observing the companion gamma ray flux because the attenuation of the gamma rays on the CMB and ISRF depends on the distance of the source.

The top panel of Fig. 11 shows the integral spectra at the Earth of neutrinos (all flavors) produced in proton-proton interactions for the two values of the maximum energy of the proton spectrum considered, for $\gamma = 2$, and $\delta = 1/2$. The bottom panel of Fig. 11 shows the corresponding gamma ray flux for these two cases and also for the case in which the gamma rays and neutrinos originate in an extragalactic source. For the extragalactic case it is assumed that the source is located at 4 Mpc from the Solar System; the attenuation in the CMB and ISRF used for the calculation corresponds to the extragalactic case of Fig. 4. Also in this case, we use $\delta = 1/2$. The maximum energy for the proton spectrum used in this case is $E_{max} = 2 \times 10^4$ TeV, but a very similar spectrum is obtained for $E_{max} = 1.2 \times 10^5$ TeV due to the sudden cutoff at ~ 100 TeV produced by the CMB and ISRF attenuation. The normalization of the spectra is chosen such that the gamma ray flux is very well observed by the different experiments. The bottom panel of Fig. 11 also shows the sensitivity of different planned or under-construction experiments: CTA (Cherenkov Telescope Array) [22], HiSCORE (Hundred**i* Square-km Cosmic ORigin Explorer) [23], HAWC (High Altitude Water Cherenkov) [24], and LHAASO (Large High Altitude Air Shower Observatory) [25]. Note that only CTA and HiSCORE are planned for the Southern Hemisphere² which is ideal for the observation of the Galactic Center.

From Fig. 11 it can be seen that, thanks to the attenuation of the gamma rays in the photon fields, it is possible to at least decide about the Galactic or extragalactic origin of the neutrino flux observed at the Earth. Moreover, in the case of a Galactic neutrino source not necessarily placed in the Galactic Center region, the measurement of the corresponding gamma ray flux can give an estimation of the distance of the source, provided that the gamma ray flux reaches energies larger than a few PeV.

It is worth noting that the test proposed here requires clear evidence of the existence of a neutrino source and a good measurement of its spectrum. Although the present IceCube data show some hints of the existence of one or more neutrino sources in the Galactic Center region, the present statistics is still poor for this type of test. This situation can change in the near future when more data are collected.

V. CONCLUSIONS

In this work we have studied in detail the shape of the gamma ray and neutrino energy spectra generated by the interaction of cosmic ray protons with ambient protons. We have considered two possible maximum energies for the proton spectrum: one consistent with the Galactic

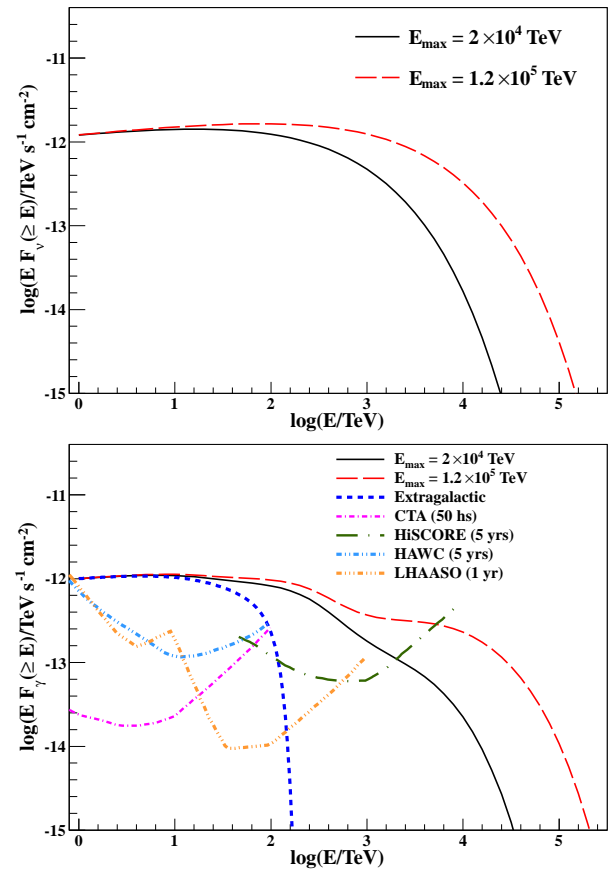


FIG. 11. Top panel: Logarithm of the integral neutrino flux multiplied by the energy as a function of the logarithm of the energy for two values of the maximum energy of the proton spectrum. Bottom panel: Logarithm of the integral gamma ray flux multiplied by the energy as a function of the logarithm of the energy for a source located in the Galactic Center for two different values of the maximum energy of the proton spectrum and for an extragalactic source located at 4 Mpc in the direction of the Galactic Center. Also shown are the sensitivity curves of different planned or under-construction experiments.

to extragalactic transition of the cosmic rays given in the second knee region and the other in the ankle region. We have studied the propagation of gamma rays and neutrinos from the source to the Earth, paying special attention to the case in which the source is located in the Galactic Center region. We have shown that the shape of the gamma ray and neutrino spectra at the Earth reflects the properties of the spectrum of protons accelerated in the sources; then the observation of these two types of secondaries can be very useful for the study of the cosmic ray sources.

We have studied the accuracy of a common approximation to infer the gamma ray spectrum from the neutrino spectra. We have found that at low energies the approximate calculation underestimates the gamma ray spectrum in less than ~ 26 % (for the four different types of proton spectra considered in this work) and that

² The CTA project consists in the construction of two observatories, one in each hemisphere, but the southern observatory will be constructed first.

at higher energies the approximate calculation overestimates the gamma ray spectrum. The differences between the approximate spectrum and the one obtained numerically are larger in the region corresponding to the end of the spectrum and increase with energy. This is due to the fact that the approximate spectrum is less steep than the one obtained numerically.

We have also discussed the existing degeneracy about the origin of neutrinos observed in the direction of Galactic Center region. We have shown that such degeneracy can be broken by observing the companion gamma ray spectrum (above a few PeV), which strongly depends on the distance to the source due to the interaction of the gamma rays with the low energy photons of the CMB and ISRF.

ACKNOWLEDGMENTS

A. D. S. is a member of the Carrera del Investigador Científico of CONICET, Argentina. This work is supported by CONICET PIP 114-201101-00360 and AN-PCyT PICT-2011-2223, Argentina.

Appendix A: Energy spectrum of cosmic ray protons

It is believed that cosmic rays are accelerated by the diffusive shock acceleration mechanism. Following Refs. [13, 14, 26] the differential energy spectrum of the accelerated particles ($n = dN/dE$) fulfills the equation,

$$\frac{\partial n}{\partial t} + \frac{\partial}{\partial E}(E r_{acc} n) = Q - r_{esc} n, \quad (\text{A1})$$

where r_{acc} is the acceleration rate, r_{esc} is the escape rate, and Q is the source term. The solution of Eq. (A1) for the stationary case ($\partial n_{esc}/\partial t = 0$) and for $Q(E, t) =$

$\dot{N}_0 \delta(E - E_0)$ is given by,

$$n(E) = \frac{\dot{N}_0}{E r_{acc}(E)} \exp \left(- \int_{E_0}^E dE' \frac{r_{esc}(E')}{E' r_{acc}(E')} \right). \quad (\text{A2})$$

The spectrum of the accelerated particles that escape from the acceleration zone is given by $n_{esc} = dN_{esc}/dEdt = r_{esc} n$.

If the diffusion coefficients downstream, k_1 , and upstream, k_2 , have the same power-law dependence with the energy of the accelerated particles, $k_1 \propto E^\delta$ and $k_2 \propto E^\delta$, the acceleration rate takes the form [13],

$$r_{acc}(E) = a E^{-\delta}. \quad (\text{A3})$$

The escape rate can also be written as [13, 14]

$$r_{esc}(E) = b E^{-\delta} + c E^\delta, \quad (\text{A4})$$

where the first term takes into account the particles that escape downstream and the second term is related to the escape of particles due to the finite size of the acceleration region [14].

From Eqs. (A2), (A3), and (A4) the energy spectrum of the escaping particles can be written as,

$$n_{esc}(E) = \frac{\dot{N}_0}{E_0} (\gamma - 1) \left(1 + \left(\frac{E}{E_{max}} \right)^{2\delta} \right) \exp \left[- \frac{\gamma - 1}{2\delta} \right] \times \left[\left(\frac{E}{E_{max}} \right)^{2\delta} - \left(\frac{E_0}{E_{max}} \right)^{2\delta} \right], \quad (\text{A5})$$

where $E_{max} = (b/c)^{1/\delta}$ and $\gamma = b/a - 1$. Therefore, Eq. (1) is obtained from Eq. (A5) by using

$$A = \frac{\dot{N}_0}{E_0} (\gamma - 1) \exp \left[\frac{\gamma - 1}{2\delta} \left(\frac{E_0}{E_{max}} \right)^{2\delta} \right]. \quad (\text{A6})$$

Note that possible energy losses suffered by the particles during the acceleration process are not taken into account in the present calculation.

-
- [1] M. Aartsen et al. (IceCube Collaboration), *Science* **342**, 1242856 (2013).
 - [2] M. Aartsen et al. (IceCube Collaboration), *Phys. Rev. Lett.* **111**, 021103 (2013).
 - [3] N. Gupta, *Astropart. Phys.* **35**, 503 (2012).
 - [4] L. Anchordoqui et al., arXiv:1306.5021 [Phys. Rev. Lett. (to be published)].
 - [5] K. Murase, M. Ahlers, and B. Lacki, arXiv:1306.3417 [Phys. Rev. Lett. (to be published)].
 - [6] M. Ahlers and K. Murase, arXiv:1309.4077 [Phys. Rev. D. (to be published)].
 - [7] A. Neronov, D. Semikoz, and C. Tchernin, arXiv:1307.2158.
 - [8] S. Razzaque, *Phys. Rev. D* **88** 081302 (2013).
 - [9] R. Aloisio, V. Berezhinsky, and A. Gazizov, *Astropart. Phys.* **39**, 129 (2012).
 - [10] I. Moskalenko, T. Porter, and A. Strong, *Astrophys. J.* **640**, L155 (2006).
 - [11] A. M. Hillas, *Proceedings of Cosmology, Galaxy Formation and Astroparticle Physics on the Pathway to the SKA* (Oxford, United Kingdom, 2006).
 - [12] M. Longair, *High Energy Astrophysics* (Cambridge University Press, Cambridge, England, 2011).
 - [13] R. Protheroe and T. Stanev, *Astropart. Phys.* **10**, 185 (1999).
 - [14] R. Protheroe, *Astropart. Phys.* **21**, 415 (2004).
 - [15] S. Kelner, F. Aharonian, and V. Bugayov, *Phys. Rev. D* **74**, 034018 (2006); *Phys. Rev. D* **79**, 039901 (E) (2009).

- [16] R. Fletcher, T. Gaisser, P. Lipari, and T. Stanev, Phys. Rev. D **50**, 5710 (1994).
- [17] A. Kappes, J. Hinton, C. Stegmann, and F. Aharonian, Astrophys. J. **656**, 870 (2007); Astrophys. J. **661**, 1348 (E) (2007).
- [18] C. Giunti and C. Kim, *Fundamentals of Neutrino Physics and Astrophysics* (Oxford University Press, Oxford, England, 2007).
- [19] P. Harrison, D. Perkins, and W. Scott, Phys. Lett. B **530**, 167 (2002).
- [20] J. Beringer et al. (Particle Data Group), Phys. Rev. D **86**, 010001 (2012) and 2013 partial update for the 2014 edition (<http://pdg.lbl.gov>).
- [21] R. Protheroe, Mon. Not. R. Astr. Soc. **221**, 769 (1986).
- [22] B. Acharya et al. (The CTA Consortium), Astropart. Phys. **43**, 3 (2013).
- [23] D. Hampf, M. Tluczykont, and D. Horns, Nuclear Instruments and Methods in Physics Research A **712**, 137 (2013).
- [24] T. De Young for HAWC Collaboration, Nuclear Instruments and Methods in Physics Research A **692**, 72 (2012).
- [25] M. Zha on behalf of ARGO-YBJ and LHAASO Collaborations, Int. J. Mod. Phys. Conf. Ser. **10**, 147 (2012).
- [26] L. Drury et al., Astron. Astrophys. **347**, 370 (1999).